Earth and Planetary Science Letters 397 (2014) 42–56

Contents lists available at ScienceDirect

Earth and Planetary Science Letters

www.elsevier.com/locate/epsl

Alpine lithosphere slab rollback causing lower crustal seismicity in northern foreland

J. Singer [a,*], T. Diehl [b], S. Husen [b,c], E. Kissling [a], T. Duretz [d]

[a] *Institute of Geophysics, Swiss Federal Institute of Technology, ETH Zurich, CH-8092 Zurich, Switzerland*
[b] *Swiss Seismological Service, Swiss Federal Institute of Technology, ETH Zurich, CH-8092 Zurich, Switzerland*
[c] *Kantonales Laboratorium Basel-Stadt, CH-4056 Basel, Switzerland* [1]
[d] *Institut des Sciences de la Terre, Batiment Geopolis, CH-1015 Lausanne, Switzerland*

ARTICLE INFO

Article history:
Received 23 December 2013
Received in revised form 29 March 2014
Accepted 1 April 2014
Available online 6 May 2014
Editor: P. Shearer

Keywords:
lower crustal earthquakes
northern Alpine foreland
slab rollback
stress transfer
high-precision earthquake locations

ABSTRACT

Beneath the northern foreland of the Central Alps deep crustal earthquakes up to magnitude 4 regularly occur in the continental lithosphere. At 20 km to 30 km depths, where most of these earthquakes are located, temperatures above 450 °C are expected. This leads to a more ductile rheology of the lower continental crust. To better understand occurrence and underlying processes of these unusual earthquakes, we homogenize and improve hypocenter locations of events in the period 1984 to 2012 using a high-precision multi-phase earthquake location method in combination with a reliable three-dimensional P-wave velocity model of the crust and uppermost mantle. With the new approach, the average uncertainty in focal depth of well-locatable earthquakes is less than ± 1 km. The homogeneously relocated hypocenters suggest a relatively uniform depth distribution throughout the lower crust. In agreement with previous studies, seismicity is entirely restricted to the crust and no evidence for seismicity in the mantle lithosphere beneath the northern Central Alpine foreland was found. The geographical distribution of lower crustal earthquakes in the foreland correlates remarkably well with the lateral extent of the European slab beneath the Central Alps where it is still attached to the European lithosphere. In addition, the directions of extensional axes derived from focal mechanisms of the deep crustal earthquakes are predominantly parallel to the Alpine front. This consistency of extensional axes can be interpreted as the result of the transferred buoyancy force of the lower crust in the subduction, transformed to a compressional force in the foreland perpendicular to the Alpine front. Existing 2-D thermo-mechanical models predict such viscous bending and stress transfer to the foreland. In our proposed model, the anomalously deep crustal seismicity is driven by stresses transferred into the foreland interrelated with the exhumation of the crust form the orogenic root caused by the rollback of the European lithosphere.

1. Introduction

In the northern Alpine foreland of Switzerland the peculiar occurrence of lower crustal earthquakes in the continental European lithosphere has long been observed and intensively discussed (Deichmann and Rybach, 1989; Deichmann, 1992; Kissling et al., 2006a; Meissner and Kern, 2008). In February 2012, a magnitude 4.2 earthquake located just above the crust-mantle boundary (Moho) at 32 km depth resumed the discussion about the origin of the lower crustal seismicity in the foreland of the Alps. Since 1984 more than 470 earthquakes were located in the lower crust within 15 km of the Moho with an average local magnitude of 2 and a maximum magnitude of ML 4.2. These deep crustal earthquakes are concentrated in the northern foreland of the Central Alps and are absent south of the Alpine front (Deichmann et al., 1999). Beneath the northern foreland of the Western and Eastern Alps little evidence for the occurrence of lower crustal seismicity exists (Fig. 1). Although most of the lower crustal earthquakes are relatively small events ($ML \leq 2$), their occurrence and spatial distribution give important insights into the rheologic and dynamic processes of the European lithosphere, engaged in the Alpine continent–continent collision. An understanding of the dynamic processes of the collision and its implication for the predominant tectonic stresses is essential for the seismic hazard assessment in the northern Alpine foreland.

* Corresponding author.
E-mail address: julia.singer@erdw.ethz.ch (J. Singer).
[1] Present address.

http://dx.doi.org/10.1016/j.epsl.2014.04.002

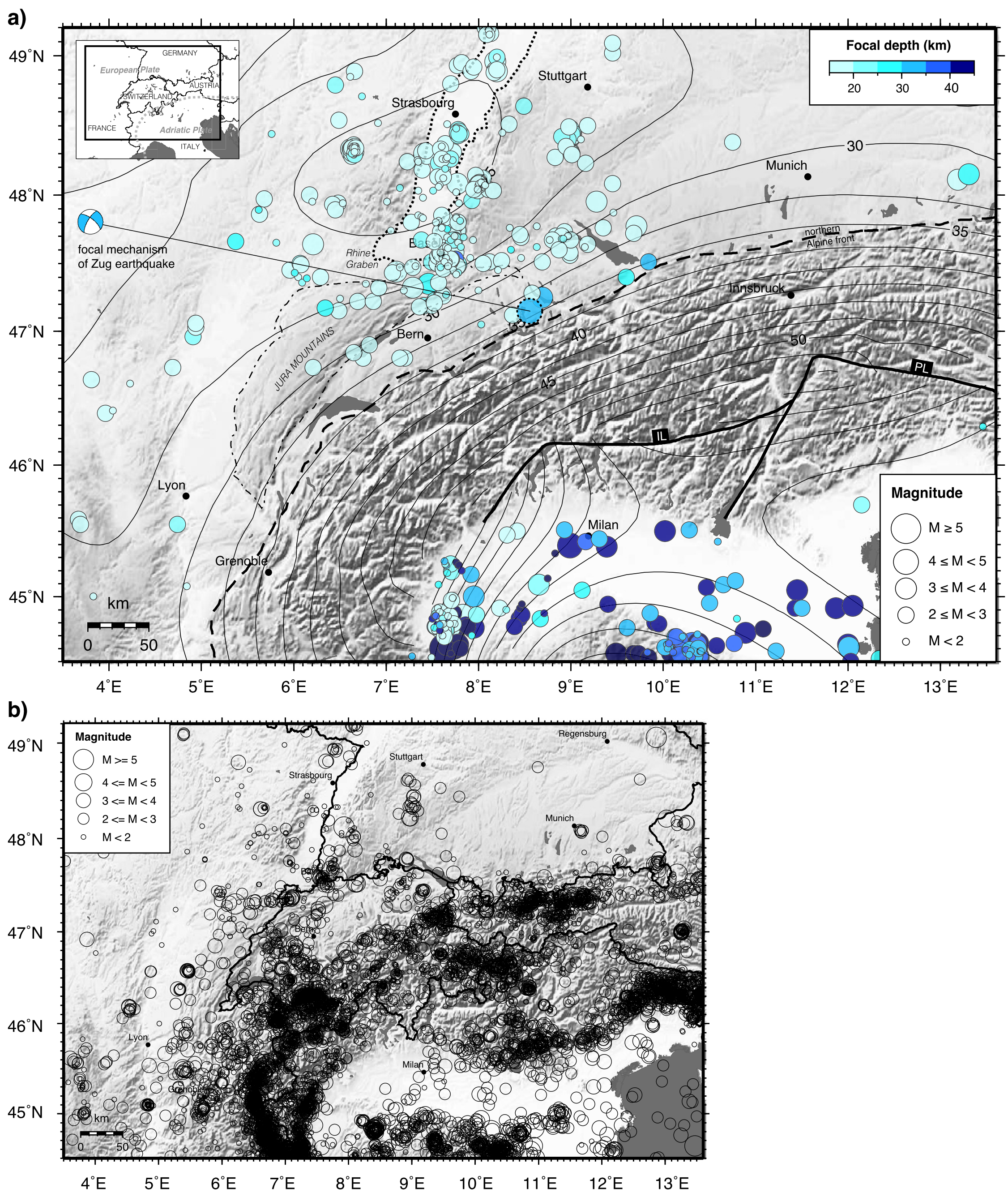

Fig. 1. Distribution of lower and upper crustal seismicity in the Alpine region as reported by the EMSC catalog for the period of 1998 to 2011. (a) Lower crustal seismicity: Earthquakes located within 15 km of the Moho are shown as circles with color indicating focal depth. The hypocenter location of the Zug earthquake on February 24, 2012 was determined by the Swiss Seismology Service (blue circle with dotted black outline). Contour lines indicate Moho depth (km) of the European respectively the Adriatic lithosphere (Wagner et al., 2012). The dotted line indicates the Rhine Graben, the dashed line the northern Alpine front (Helvetic front) and the dot-and-dashed line the extent of the Jura Mountains. IL: Insubric Line; PL: Periadriatic Line. (b) Corresponding upper crustal seismicity distribution (focal depth < 20 km and hypocenter distance to the Moho >15 km).

In the continental lithosphere the seismicity is generally confined to the brittle upper crust (Chen and Molnar, 1983; Chen, 1988; Maggi et al., 2000a; Scholz, 2002; Jackson, 2002). Earthquakes located in the lower crust like in the northern Alpine foreland or even in the mantle lithosphere outside subduction zones are rare. Besides the Alps such deep crustal earthquakes were recorded beneath the Tien Shan, northern India, East Africa, along the Oman Line (Maggi et al., 2000b) or Mongolia–Baikal (Jackson et al., 2008). From laboratory experiments, the key controlling factor, determining whether deformation of the lower continental crust is brittle or ductile is temperature (Chen et al., 2012). The supposed upper temperature limit for the brittle crust is around 300 – 400 °C and around 600 – 700 °C for the mantle (Chen et al., 2012). At 20 km to 30 km depths where most of the lower crustal earthquakes in the northern Alpine foreland occur, however, higher temperatures and a ductile rheology are expected (Deichmann and Rybach, 1989; Okaya et al., 1996). In contrast, Holliger and Levander (1994) and Meissner and Kern (2008) proposed a strong European lower crust based on a 'corset model' of thin mafic to ultramafic, sill-like intrusions to explain both the high-reflectivity of the laminated lower European crust and its seismicity. The distinct geographical distribution of these earthquakes and the origin of the required high tectonic stress, however, remain unresolved. The orientation of the regional stress field of the northern foreland of the Central Alps is dominated by an arc-parallel extension (ENE–WSW) and arc-perpendicular compression (NNW–SSE) (Delacou et al., 2004; Kastrup et al., 2004). Within the orogen belt of the Central and Western Alps, the stress pattern is different with a dominant arc-perpendicular extension and thus predominant normal faulting (Sue et al., 1999; Delacou et al., 2004; Sue et al., 2007b; Marschall et al., 2013).

The occurrence of high-pressure fluids as an explanation for the observed lower crustal seismicity were suggested by Deichmann and Rybach (1989), Deichmann (1992). Nevertheless, the reason for the release of such fluids peculiar in this region of the northern Alpine foreland remains unclear. An association with the Alpine orogeny would imply that fluids are presented as well in the crustal root of the Alps. Consequently, lower crustal earthquakes are expected to occur behind the northern Alpine front beneath the Alps, but no observation of lower crustal seismicity exists in this region (Fig. 1a). Although, fluid overpressure might be well causing seismic swarm activity in the upper crust (Leclère et al., 2013) and may play a general role in the generation of lower crustal earthquakes, its role as primary source for the anomalous lower crustal seismicity in a specific subregion of the northern Alpine foreland remains purely speculative.

Hypocenter locations in the earthquake catalog of the Swiss Seismological Service have been routinely derived with different location algorithms and velocity models. The assessment of location uncertainties are non-consistent and the precision varies strongly. As a consequence, the focal depth distribution of events in this catalog is relatively diffuse, in particular for the lower crustal seismicity in the northern Alpine foreland. It is unclear whether the large vertical scattering is due to systematic uncertainty variations or different location methods. In any case, the depth distribution of hypocenters is important in the assessment of underlying processes, like metamorphic reactions or stress concentrations. Furthermore, considering the rheological differences between lower crustal and uppermost mantle, earthquake locations above or below the Moho are essential. Hence, accurate and precise hypocenter locations with a uniform uncertainty assessment are needed for all recorded lower crustal earthquakes. To obtain improved and homogeneous hypocenter locations, we apply the new high-precision multi-phase earthquake location method of Wagner et al. (2013). This location algorithm includes a realistic 3-D seismic velocity model for the Central Alps and, in particular, the 3-D topography of the Moho in combination with multi-phase ray-tracing of first and later arriving crustal phases.

In this study, we first summarize the high-precision 3-D multi-phase earthquake relocation method of Wagner et al. (2013). This approach is then applied to the heterogeneously located earthquake catalog of the Swiss Seismological Service (ECOS-09 with an extension to 2012). The newly derived distribution of focal depths and characteristics of focal mechanisms are analyzed with respect to large-scale lithosphere structures. We propose an anomalously high tectonic stress in the lower crust of the northern foreland of the Central Alps as the primary reason for the peculiar occurrence of lower crustal seismicity in this region. Finally we compare our model with recently published 2-D numerical continent–continent collision models (Duretz and Gerya, 2013).

2. High-precision multi-phase earthquake relocation in a 3-D velocity model

The correct identification of first and later arriving seismic phases in seismogram records adds important constraints on the earthquake location problem (e.g. Deichmann, 1987; Quin and Thurber, 1992; Engdahl et al., 1998; Wagner et al., 2013). For instance, earthquakes can be unambiguously identified as crustal events if Pg (direct), PmP (Moho-reflected) and Pn-phases (critically refracted at the Moho) are observed in travel-time reduced record sections (Fig. 2) (Diehl et al., 2009b). To accurately determine the focal depth of local and regional earthquakes, differential times between crustal phases like Pg and PmP or Pg and Pn can be used (e.g. Garcia Fernandez and Mayer-Rosa, 1986; Deichmann, 1987; Kastrup et al., 2007; Wagner et al., 2013). To make use of these later arriving P-phases in an earthquake location algorithm, forward solvers have to be extended to precisely trace PmP and Pn ray-paths in complex elastic media. The computation of realistic PmP and Pn travel times also requires reliable knowledge of Moho topography and the presence of a first-order discontinuity in the seismic velocities across the Moho. Such a sharp velocity gradient is commonly not present in 3-D models derived from standard local earthquake travel-time tomography due to constraints in the parameterization of the inversion grid (e.g. Kissling et al., 2001; Husen et al., 2003).

A crustal 3-D P-wave velocity model appropriate for the precise forward calculation of Pg, Pn and PmP travel times in the Alpine region was compiled by Wagner et al. (2012) by combining models from local earthquake tomography (LET) (Diehl et al., 2009a) and controlled source seismology (CSS) (Waldhauser et al., 2002). The combination of both models, including the interpolation of the Moho interface for the entire model space, results in an improved 3-D Moho topography of the Alpine region and a 3-D P-wave velocity model with a first-order discontinuity at the Moho (Wagner et al., 2012). Seismic velocities are defined on a 2 km vertically and horizontally spaced grid and travel-time tables for Pg, Pn and PmP phases are calculated for each seismic station using the multistage Fast Marching Method (FMM) with separate computational domains (Rawlinson and Sambridge, 2004).

The earthquake location problem is solved by a nonlinear, probabilistic approach implemented in the NonLinLoc algorithm (http://alomax.free.fr/nlloc/), which was extended to the proposed multiphase inversion (Wagner et al., 2013). NonLinLoc determines a complete probabilistic solution of the location problem including a posterior probability density function (PDF) of the earthquake hypocenter location. The PDF of the location solution includes uncertainties due to observation errors, geometric distribution of the seismic stations and calculation errors of the predicted travel times (Lomax et al., 2000). To determinate the PDF a 3-D global search algorithm is applied. As a misfit function we used the equal differential time function with origin time weighting (EDT-OT-WT) together with the Oct-tree Importance Sampling as a search algorithm. The EDT-OT-WT misfit function is robust and less sensitive in the case of outliers compared to the L2-misfit function (Lomax, 2005). Since secondary phases outliers are more likely due to misidentification a robust misfit function like the EDT-OT-WT is needed.

For the relocation with the multi-phase procedure of Wagner et al. (2013) all picked phases require an exact identification (Pg, Pn or PmP). If Pg-phases are identified in combination with Pn- or PmP-phases the earthquake source can be preliminary determined above the Moho; this limits the search volume to the crust. Earthquake location algorithms using the finite difference (FD) forward solver, assume any pick as the first arriving phase. If these picks are used in combination with models lacking a first-order discontinuity at the Moho, hypocenters can be mistakenly located beneath the Moho in the mantle lithosphere despite clearly identified Pg- or PmP-phases. For the relocation of lower crustal seismicity we used only P-phase arrivals and no S-phases. To include S-phase arrivals in the hypocenter determination an S-wave velocity model with a resolution comparable to the 3-D P-wave velocity model would be required. Such an S-wave model, however, is not yet available. Furthermore, a constant Vp/Vs – ratio is

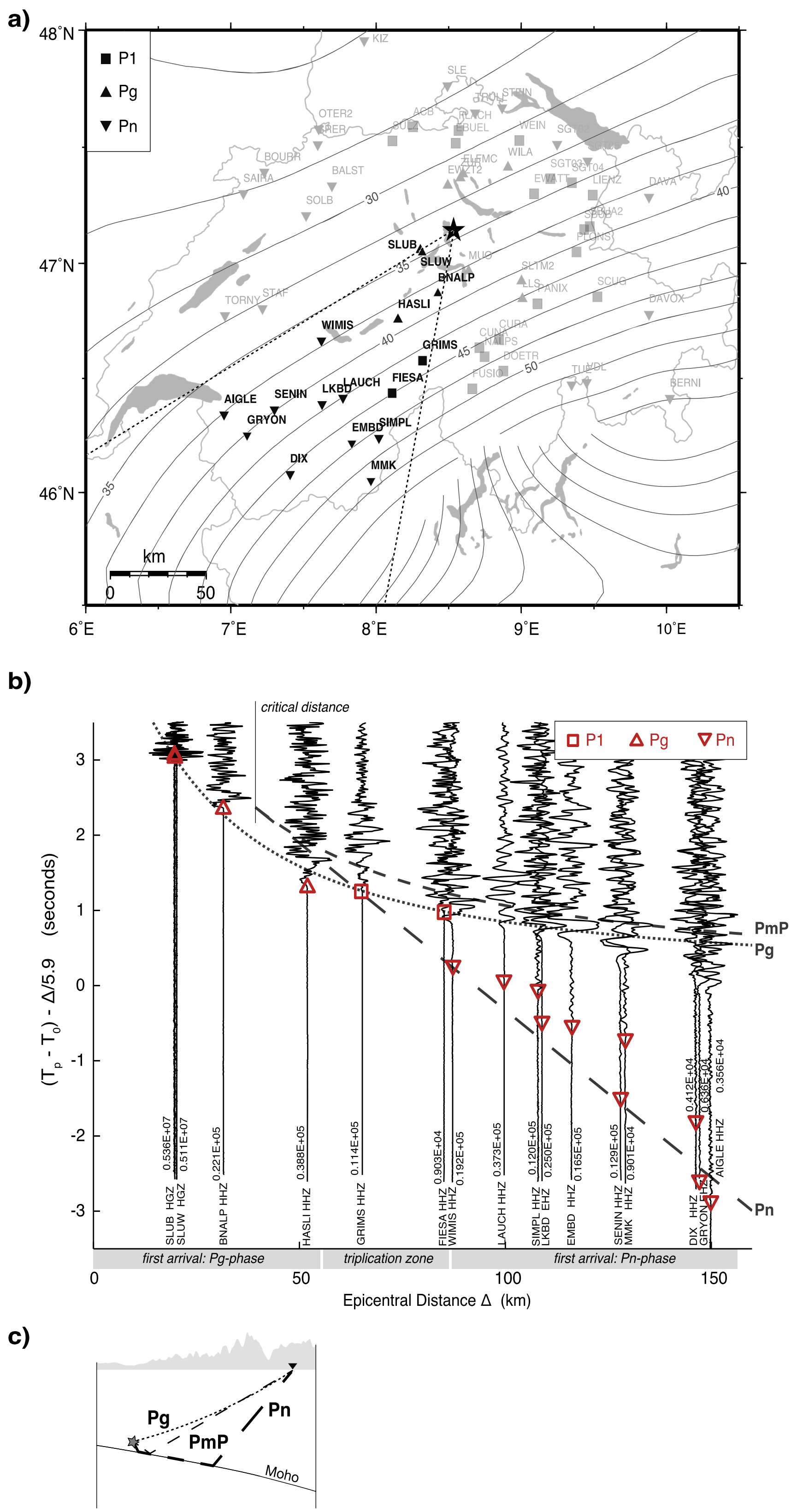

Fig. 2. Identification of main crustal P-phases with travel-time reduced record sections. (a) Map of seismic stations with routinely picked P-phases by the Swiss Seismological Service for the Zug earthquake on February 24, 2012 at 00:32 (UTC) with ML 3.5 at 32 km depth. Epicenter is indicated with star. Stations with phase picks not shown in (b) are shown with gray colors. Black contour lines represent the Moho depth (km) of the European respectively Adriatic plate (Wagner et al., 2012). (b) Velocity reduced record section. The crustal reduction velocity is 5.9 km/s. Synthetic travel time curves for Pg (dotted), Pn (dashed) and PmP (dashed) are based on a simplified 1-D lithospheric model with Moho depth at 34 km. For the synthetic Pn-travel time curve an average mantle velocity of 8 km/s is used. The crustal P-wave velocity in the model is 5.9 km/s like the reduction velocity. For this event no PmP-phase picks were used for the localization. (c) Schematic diagram of travel time paths of main crustal P-phases from a lower crustal earthquake.

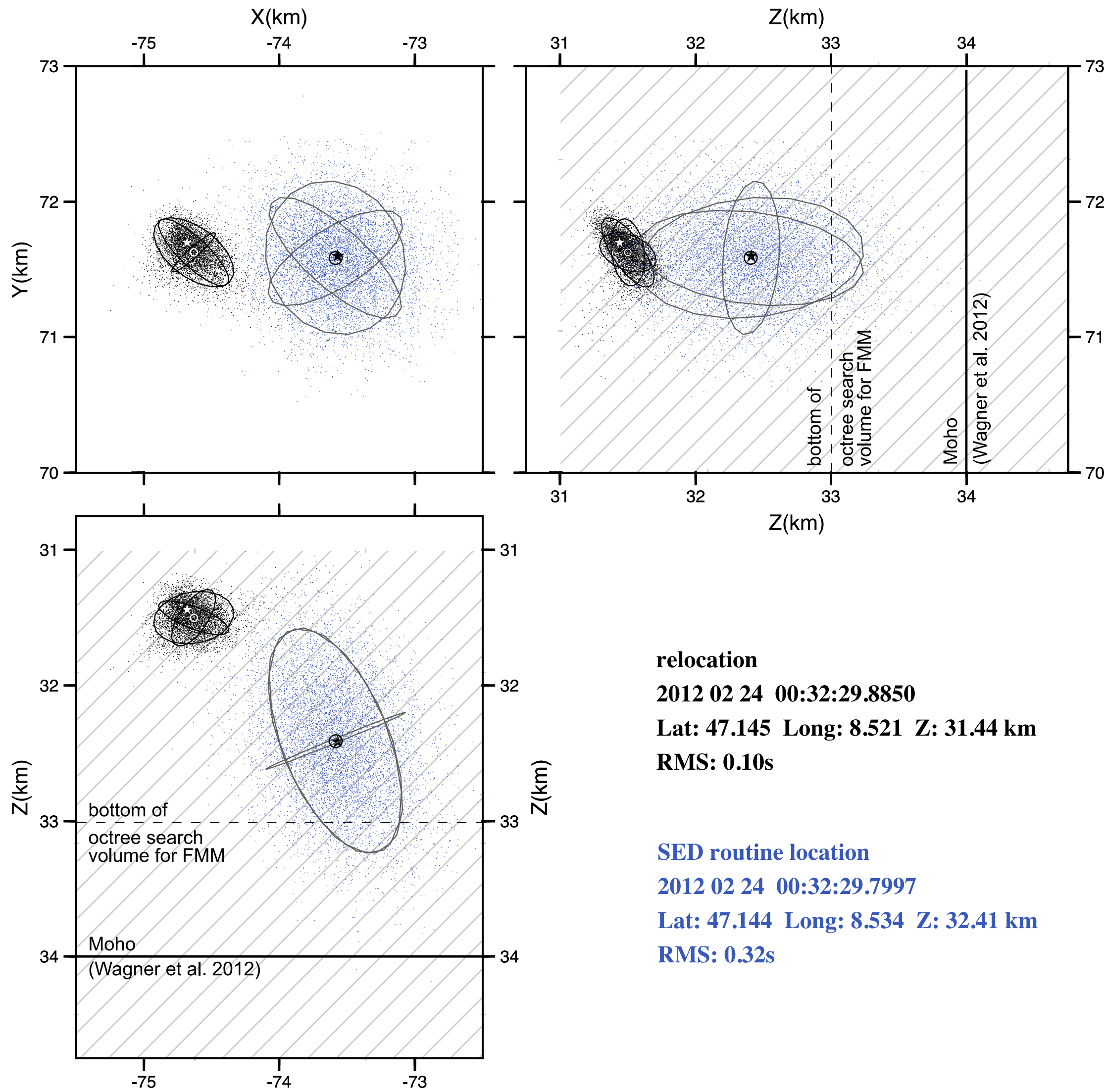

Fig. 3. Density scatter plot of PDF (Lomax et al., 2000) of the lower crustal Zug earthquake of February 24, 2012. Black dots show newly derived high-precision location and gray dots show the routinely derived location with using finite different forward-solver and a 3-D velocity model without a first-order discontinuity at the Moho (Husen et al., 2003). The black and white stars present the maximum likelihood hypocenter location and black/white circles the Gaussian estimate of the hypocenter locations. Black/gray lines indicate the projection of the 68 % confidence ellipsoid. The minimum Moho depth uncertainty of ± 3 km is shown by the striated area. Thin black line marks Moho depth at newly derived epicenter location and black dashed line bottom of the Oct-tree search volume at this epicenter location.

not appropriate for the Alpine region to define an S-wave model with comparable resolution. The Vp/Vs – ratio varies significantly between different tectonic units along the Alpine arc (Lombardi et al., 2008).

In Fig. 3 an example of the PDF of a relocated lower crustal earthquake is shown using the new multi-phase location method of Wagner et al. (2013). The earthquake occurred close to the city of Zug (Fig. 2a) on February 24, 2012 with a local magnitude of 3.5. Compared to the routine location of the Swiss Seismological Service (SED) without a first-order discontinuity in the 3-D velocity model at the Moho and an FD forward-solver (Husen et al., 2003), the precision with respect to the Moho of the hypocenter improve significantly (Fig. 3). Although the number of phase observations is high (75 phases) and the azimuthal station coverage is very good for the routine SED location (azimuthal gap in station coverage is 21°), the new multi-phase location using fewer phases (46 identified P-phases) and a larger azimuthal gap in station coverage of 38° still exhibits a higher precision in focal depth (less than 1 km) and epicenter (Fig. 3). The epicenter is slightly shifted westwards by around 1 km and the focal depth is located around 1 km above the SED routine hypocenter (Fig. 3).

3. Lower crustal seismicity in the northern Alpine foreland

3.1. Earthquake relocations

In total our earthquake catalog covers the period between January 1984 and September 2012 and combines the earthquake catalog of Switzerland (ECOS-09) (Fäh et al., 2011) and additional earthquakes after 2008 from the SED earthquake bulletin. It contains 471 lower crustal earthquakes within 15 km of the Moho surface (Wagner et al., 2012). The combined catalog is denoted ECOS-09(12) in the following. The thickness of the European lower crust is assumed to be about 12 km as suggested by a characteristic band of high-reflectivity in the European crust extended from the Alps towards the northern foreland (Holliger and Kissling, 1992; Ye et al., 1995). The 15 km wide band used for the selection accounts for potential errors in focal depths and includes lower crustal earthquakes, which are mistakenly located in the middle crust by the ECOS-09(12) catalog.

From the 471 initial lower crustal events, 152 well-locatable earthquakes, with a maximum azimuthal gap in station coverage of 180° and a minimum of 10 P-phase picks in the ECOS-09(12) location have been selected for the further relocation. For the 152 selected events we revised the identification of P-phases with the help of reduced record sections (e.g. Deichmann and Rybach, 1989; Diehl et al., 2009a) as demonstrated in Fig. 2. For each crustal P-phase (Pg, Pn and PmP) a characteristic reduced-travel-time curve exists as shown in Fig. 2b and corresponding phase picks align along these curves. Obvious misidentifications of phase picks outside the triplication zone (Fig. 2b) can be corrected and otherwise unknown phase picks identified. To account for the dipping Moho (Wagner et al., 2012) and its influence on Pn and PmP travel times, we used reduced record sections with different azimuthal coverage to simplify the revision of P-phase picks (Fig. 2). If required we re-identified P-phases. We did not, however revise the timing of P-phase arrivals reported in the SED bulletin data, nor did we add additional P-phase picks. Altogether the revised earthquake data show 1687 Pg-phases, 840 Pn-phases and 36 PmP-phases. All earthquakes show direct (Pg) and refracted P-phases (Pn) or even secondary P-phases such as PmP. Therefore, all 152 well-locatable earthquakes are of crustal origin and none of them occurred in the European mantle lithosphere.

Only five non-well-locatable events are located in the European mantle lithosphere in the ECOS-09(12) catalog by other location methods (e.g. FD travel time computation using a 3-D P-wave model, Husen et al., 2003), with several kilometers of uncertainties in the focal depth. In combination with a minimum uncertainty of ± 3 km in the Moho depth (Wagner et al., 2012; Waldhauser et al., 1998) these events can also be located in the crust as documented by Diehl et al. (2009a). The general observation of an aseismic European mantle agrees with earlier studies (e.g. Deichmann and Rybach, 1989; Deichmann, 1992; Diehl et al., 2009a).

With the re-identified P-phase arrivals of the 152 earthquakes we then relocated the events with the new multi-phase location procedure implemented in the NonLinLoc software (Wagner et al., 2013) to obtain high-precision hypocenters. The quality of the hypocenter solution was assessed by the heterogeneity of the location PDF (Lomax et al., 2000). Earthquakes were not taken into account for our best-locatable earthquake catalog when one or more of the following criteria apply: the PDF exhibits several local maxima; distance between expected and the maximum likelihood location (Lomax et al., 2000; Husen et al., 2003) exceeds 4 km; an unusually large extent of more than 10 km in the 68 % confidence ellipsoid of the PDF; or a scatter volume of the PDF greater than several km^3.

Finally, the newly derived catalog of lower crustal seismicity includes 104 best-locatable lower or middle crustal earthquakes beneath the northern foreland of the Central Alps. Compared to the ECOS-09(12) catalog, the newly derived 104 hypocenters differ on average by about ± 1.1 km and do not show a systematic shift, neither in epicenter nor in focal depth. All events are confined to the European lower or middle crust.

Fig. 4a shows the epicenters of the relocated earthquakes. Although the catalog of relocated lower crustal earthquakes contains only about 20 % of the lower crustal seismicity reported in the ECOS-09(12) catalog, the characteristics in the spatial distribution are comparable. The majority of lower crustal seismicity is clustered in the eastern and central Swiss Alpine foreland and at the southern end of the Rhine Graben. Towards the Western Alps, seismicity in the lower European crust diminishes and magnitudes are generally smaller. To the Southeast, the lower crustal seismicity reaches the maximum depth of 33 km and abruptly ends at the Alpine front (Figs. 4a and 4b).

In some regions in the foreland the lower crustal earthquakes tend to occur in spatial clusters like in the region of Zug (Figs. 4a and 4b), as observed in earlier studies (Deichmann, 1992). Before the ML 4.2 Zug earthquake on February 11, 2012 other lower crustal earthquakes occurred in this area with similar hypocenter locations, like the ML 3.2 earthquake on October 23, 1997 at 32 km depth. Other than these clusters at varying depths and distance to the Alpine front (Figs. 4a and 4b), neither streaks of seismicity nor clustering at certain depth contours indicating a bimodal distribution within the lower crust were imaged by the relocated earthquakes (Fig. 4b). Furthermore, Ye et al. (1995) and Diehl et al. (2009a) showed that the P-wave velocity in the lower crust is in general homogeneous beneath the northern foreland of the Central Alps and neither the focal depth distribution nor the lateral distribution of the lower crustal seismicity can be correlated with certain P-wave velocity changes.

The major improvement resulting from the application of the systematic multi-phase relocation procedure compared to routinely used methods is the homogeneous and consistent location approach and the high-precision determination of focal depths, comparable now to the epicenter precision. Most of these earthquakes have a vertical uncertainty, measured from the vertical projection of the 68 % confidence interval of the location PDF, of less than ± 1 km similar to the epicenter uncertainties (Fig. 5).

The derived precision in focal depths allows a resolution of 2 km to analyze the seismicity-depth distribution. Generally, the focal depth distribution of the relocated hypocenter locations suggest a rather uniform focal depth distribution throughout the lower crust relative to the 3-D Moho model of Wagner et al. (2012), but with a distinct peak at 10 km to 12 km above the Moho (Fig. 6). This layer of enhanced seismicity can be interpreted as the transition zone between upper and lower crust (Conrad discontinuity), a potentially weakness zone in the crust favoring brittle failure. A similar peak in seismicity, however, at 8 km to 10 km above the Moho is also apparent in the subset of well-constrained ECOS-(09)12 locations (Fig. 6).

3.2. Focal mechanisms

The tectonic stress regimes and possible differences between upper and lower crust are derived from the analysis of available earthquake focal mechanisms published by Kastrup et al. (2004), Deichmann (2012), Marschall et al. (2013) and Diehl et al. (2013). We compared the style of faulting and the orientation of P- and T-axes in the upper and lower crust. The compiled catalog of focal mechanisms comprises 119 solutions of earthquakes between 1976 and 2012 for the northern foreland of the Central Alps, which yield a sufficient number of first motion polarities of P-wave and azimuthal distribution on the focal sphere to unambiguously determine the fault planes. All focal mechanisms have been deduced from fitting P-wave first-motion polarities with take-off angles either derived from 2-D ray-tracing of Pg- and Pn-phases (e.g. Garcia Fernandez and Mayer-Rosa, 1986; Deichmann, 1987; Deichmann and Rybach, 1989) or FD ray-tracing using a 3-D P-wave model (Husen et al., 2003). As hypocenter locations differ less than 1.1 km and the velocity model is identical in the source region, differences in take-off angles between the compiled focal mechanism earthquake catalog and our newly-derived hypocenters are negligible.

Within the focal mechanism catalog 51 mechanisms are located in the lower crust (distance to Moho $\leq$ 12 km) and 68 located in the upper crust (distance to Moho $>$ 12 km) of the northern Alpine foreland of the Central Alps. In Fig. 7a all mechanisms are shown as beach-ball symbols color-coded by distance

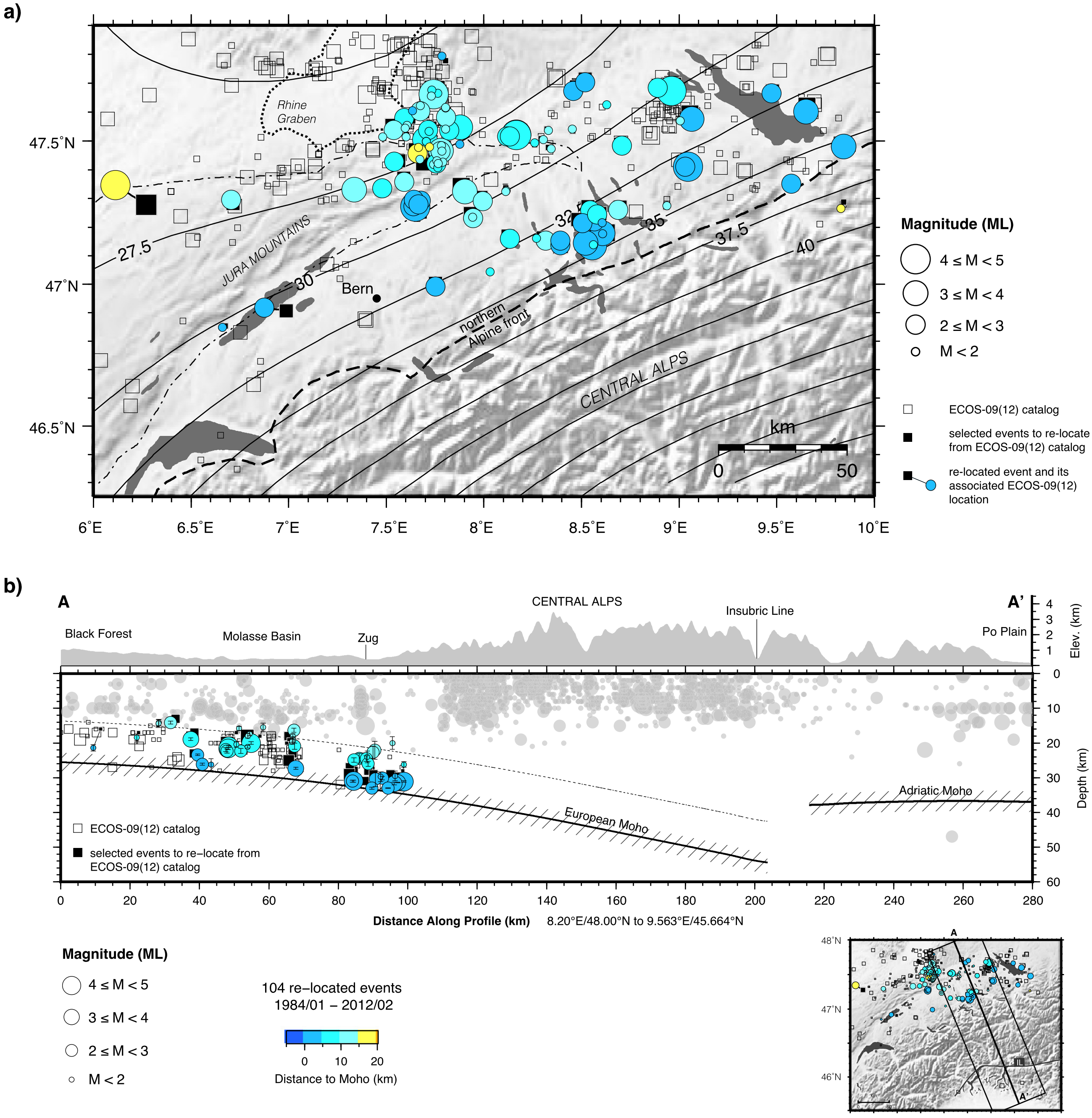

Fig. 4. Hypocenter map of relocated lower crustal earthquakes compared to hypocenters of the ECOS-09(12) catalog. (a) Map with relocated high-precision epicenter distribution of well-constrained lower crustal earthquakes (colored) and their corresponding ECOS-09(12) locations (black squares connected with black lines to newly derived epicenters). All earthquakes of the ECOS-09(12) located within 15 km of the Moho are shown as open squares with same magnitude scale like the circles. Black contour lines represent the Moho depth (km) of the European lithosphere (Wagner et al., 2012). Contour interval is 2.5 km. The northern Alpine front (Helvetic front) is indicated with the dashed line, the Rhine Graben is outlined by the dotted line and the Jura Mountains by the dot-and-dashed line. (b) Vertical cross-section approximately perpendicular to the strike of the Central Alps as indicated in map view. Colored circles represent relocated hypocenters connected to the corresponding ECOS-09(12) locations (black solid squares) with a line. Uncertainties in focal depths are presented with vertical error bars for each relocated hypocenter. Open squares represent all remaining lower crustal earthquakes within 12 km distance to the Moho of the ECOS-09(12) catalog but not included in the newly derived earthquake catalog. With transparent gray circles all other earthquakes of the ECOS-09(12) catalog within 45 km distance to the profile line are shown. The striated areas around the Moho (solid black line) represent the minimum ±3 km uncertainty of the Moho depth (Waldhauser et al., 1998; Wagner et al., 2012).

to the Moho. Between the upper and lower crust no major differences in focal mechanisms appear, strike-slip mechanisms are dominated throughout the crust with a compressional orientation consistent with the characteristic regional stress field in the Alpine foreland (NNW–SSE and an ENE–WSW oriented extension) (Delacou et al., 2004; Kastrup et al., 2004). Besides these strike-slip mechanisms a significant number of earthquakes in the upper and lower crust (∼10 %) indicates normal faulting mechanisms.

Although normal faulting and strike-slip mechanisms have in principle different fault planes, the underlying tectonic stress regime for both mechanisms is similar for the extensional T-axes. The orientation of these T-axes is consistent with the regional ENE–WSW trend in the northern foreland of the Central Alps

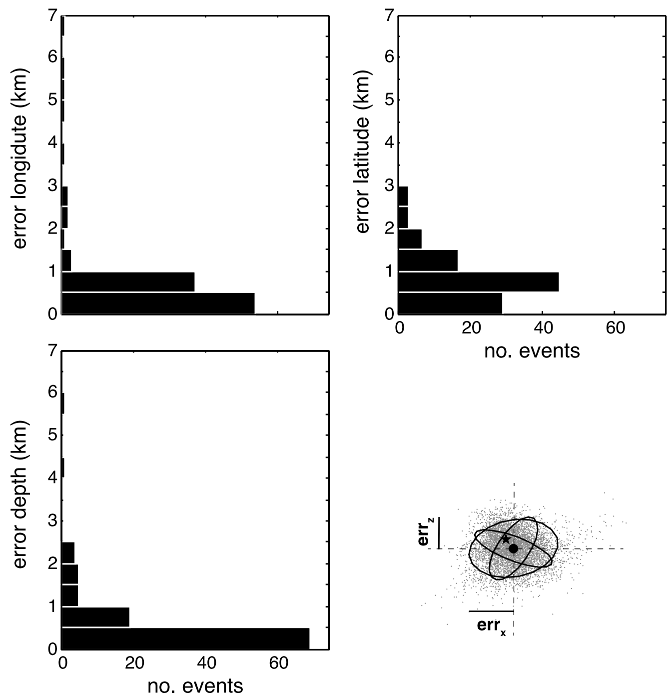

Fig. 5. Histograms of uncertainties of relocations shown in Fig. 4a projected onto (a) longitude, (b) latitude and (c) focal depth. Uncertainties in hypocenter locations (longitude, latitude and depth) correspond to the projection of the 68 % confidence ellipsoid of the posterior probability density function (PDF) as demonstrated in the lower right corner for longitude and depth.

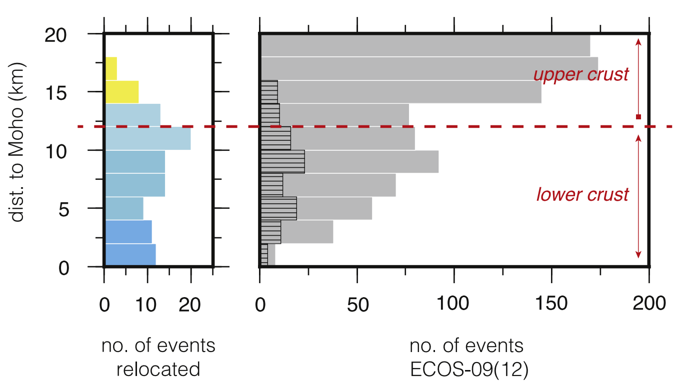

Fig. 6. Histogram of focal depths relative to the Moho depth beneath each event. Colored stacks on the left show the high-precision relocated catalog. On the right, the distribution of the ECOS-09(12) is shown in gray for all events of the ECOS-09(12) catalog and with black stripped stacks for those corresponding to the relocated events shown on the left. The lower-upper crustal boundary, indicated with the red dashed line, is defined at 12 km above the Moho (Holliger and Kissling, 1992).

(Fig. 7b, right). Only the compressional P-axes of the normal faulting events differ in azimuth and plunge from the ones seen in the strike-slip mechanisms. Azimuth and plunge of the P-axes show a higher variability (Fig. 7b, left) compared to the T-axes throughout the crust (Fig. 7b, right). In contrast to the similarity in focal mechanisms for the upper and lower crust, the corresponding T-axes of the normal and strike-slip faulting mechanisms have a higher consistency in azimuth and plunge in the lower crust than in the upper crust (Fig. 7b, right). This trend is also observed for the azimuth of the P-axes in Fig. 7b, however, not for the plunge of the P-axes (Fig. 7b). In general, focal mechanisms of lower crustal earthquakes show greater consistency in the T- and P-axes compared to the more variable axes of focal mechanisms in the upper crust. The high consistency of the extensional T-axes is a predominant feature of all focal mechanisms throughout the crust, but is especially pronounced for events in the lower crust.

3.3. Lower crustal seismicity and its geographical relation to the Alpine lithospheric structure

The high-resolution teleseismic tomography of Lippitsch et al. (2003) has imaged a strong non-cylindrical lithospheric slab structure within the upper mantle beneath the Alpine arc, with opposing subduction zones in the Eastern Alps and Western–Central Alps (Fig. 8a). Beneath the Central Alps the slab rollback of the European lithosphere controls the large-scale lithospheric dynamics (Kissling, 2008). In the Western Alps, the European mantle lithosphere slab is already detached (Fig. 8a) (Lippitsch et al., 2003; Kissling et al., 2006b; Kissling, 2008). Towards the northeast of the Western Alps, Champagnac et al. (2007) and Serpelloni et al. (2013) suggest that the subsequent increase in surface topography and erosion rates can be correlated with the recent isostatic rebound of the lithosphere. In addition, widespread extension in the internal zone of the Western Alps was documented by focal mechanisms of earthquakes and GPS measurements (Sue et al., 2007a) and related to a slab break-off (Sue et al., 2007b). This includes a possible tear propagation of the slab detachment in this region as shown in by the upper mantle structure in Fig. 8a.

To compare the entire geographical distribution of lower crustal seismicity in the northern foreland of the Alpine arc with the large-scale lithospheric structures, we analyzed focal depths reported in the regional earthquake catalog of the European-Mediterranean Seismological Centre (EMSC). The EMSC catalog includes earthquakes over a 13 year period from January 1, 1998 to July 31, 2011. The EMSC collects source parameters and phase picks of 65 seismological networks in Europe and automatically merges this data to produce automatic locations using 53 local velocity models provided by the local networks (Godey et al., 2006). As a consequence of the location approach of the EMSC catalog, we expect hypocenters to be determined less precisely compared to our relocations in the northern foreland of Switzerland. Nevertheless, the EMSC earthquake catalog allows a qualitative summary of the regional distribution of lower crustal seismicity in the northern foreland of the Alpine arc.

The clustering of lower crustal seismicity in eastern Switzerland is also apparent in the EMSC catalog (Fig. 8a). To the West, lower crustal earthquakes in the northwestern foreland of the Western Alps are rare. East of 10°E, towards the northern foreland of the Eastern Alps the lower crustal seismicity shuts down. Generally, the occurrence of lower crustal earthquakes in the northern foreland correlates well with the gently to steeply dipping European slab beneath the Central Alps (Fig. 8b, middle) with the exception of the seismicity in the Rhine Graben region (Fig. 8b, left). The Rhine Graben is an extensional graben structure in central Europe with a pronounced crustal and lithosphere thinning (Dèzes et al., 2004) and pre-existing deep faults, which dates from the end of rifting in the early Miocene while volcanism continued until as recently as 14 Myr ago (Wilson and Downes, 2006).

4. Discussion

4.1. Lower crustal seismicity in the Central Alps

The occurrence of lower crustal earthquakes in the northern Alpine foreland and their source properties provide important insights into the mechanical strength of the continental lithosphere as intensively discussed for other orogenic regions by Maggi et al. (2000b), Jackson (2002) and Jackson et al. (2008).

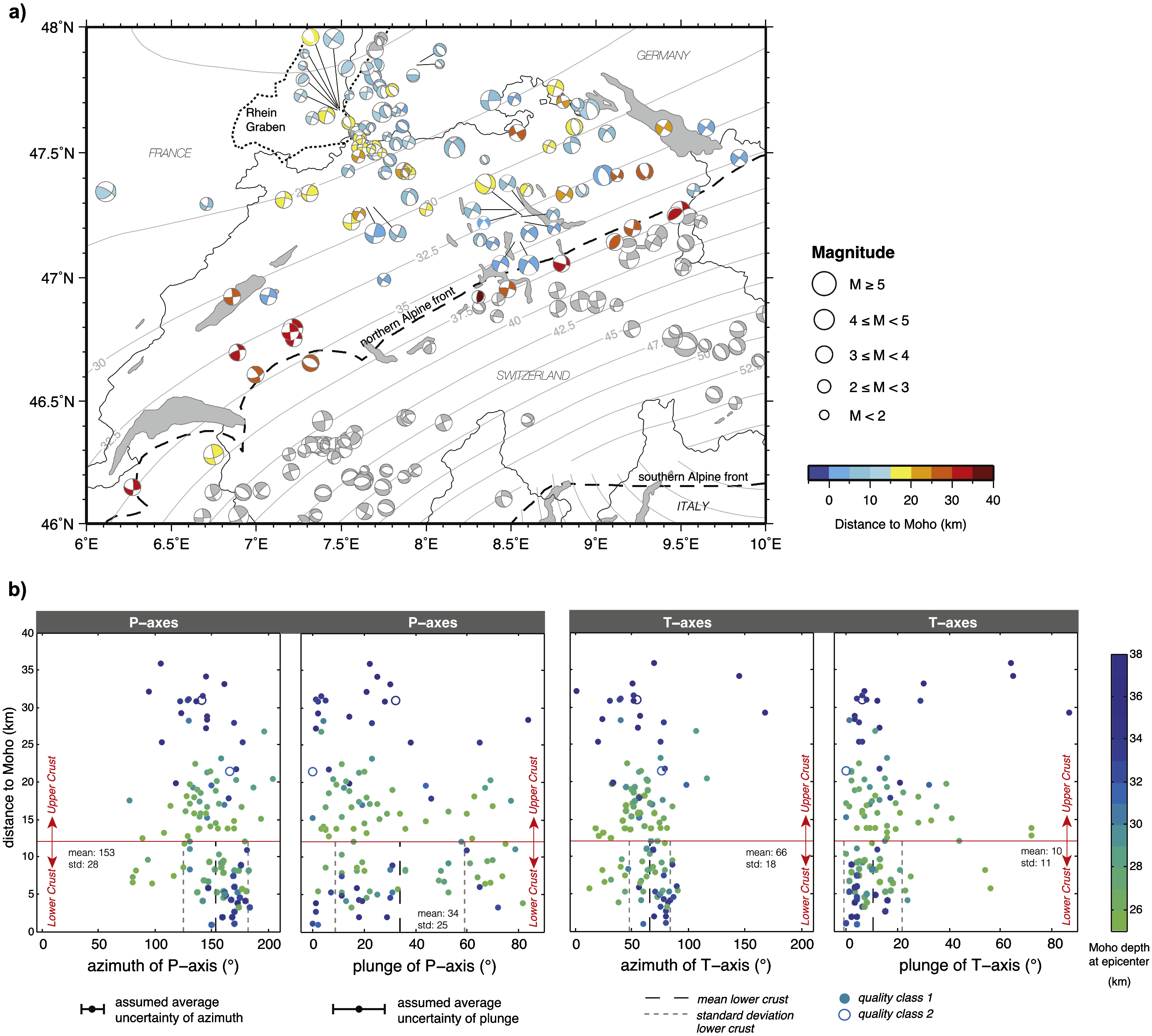

Fig. 7. Focal mechanisms in the greater region of Switzerland and their corresponding orientation of the P-/T-axes. (a) Map of focal mechanisms of lower crustal earthquakes with fault plane solutions (lower hemisphere, equal area projections) (Kastrup et al., 2004; Deichmann, 2012; Marschall et al., 2013; Diehl et al., 2013). Colored focal mechanisms correspond to earthquakes in the northern Alpine foreland and are analyzed in detail in (b). Gray focal mechanisms represent earthquakes in the upper crust where the Moho depth is deeper than 37.5 km or less than 27 km and therefore outside the northern Alpine foreland of the Central Alps. Contour lines represent the Moho depth (km) of the European and the Adriatic lithosphere (Wagner et al., 2012). (b) Orientation of P-/T-axes of colored focal mechanisms shown in (a). On the left side, azimuth and plunge of the P-axes with distance to Moho. Colors indicate the Moho depth at the epicenter of each earthquake. On the right side, azimuth and plunge of the respective T-axes of the focal mechanisms. Azimuths of P-/T-axes larger than 180° are corrected by 180° to avoid a bias in the azimuth orientation. All focal mechanisms are double couple solutions. Solid dots represent well-constrained P-/T-axes (quality class 1) and circles focal mechanisms which are less well-constrained (quality class 2).

Besides information on the strength and rheologic behavior of the lithosphere, the presence or absence of earthquakes are fundamental observations to assess dynamics and tectonic stresses in a continent–continent collision. Based on the systematic reassessment of deep earthquakes in the northern Alpine foreland including a consistent uncertainty determination with a high-precision multi-phase location method (Wagner et al., 2013), we can restrict all well-locatable earthquakes to the crust and confirm the uncommon lower crustal seismicity in the European continental lithosphere beneath the northern foreland of the Central Alps.

Previous studies of Deichmann (1992) and Deichmann and Rybach (1989) with a limited number of lower crustal earthquakes in the northern foreland recorded between 1984 to 1990 explained brittle failure in the lower crust with the existence of high-pressure fluids under near-lithostatic pressure. Although fluid overpressure might play a role in the generation of lower crustal earthquakes, its role as primary cause for the anomalous seismicity in a specific subregion of the northern Alpine foreland remains speculative. Based on a tectonic-petrological study, Holliger and Levander (1994) and Meissner and Kern (2008) proposed a 'corset model' representing the mechanics of the lower continental crust to explain both the high-reflectivity of the laminated lower European crust and the apparent contradiction between the existence of earthquakes in a hypothetically rather ductile and weak

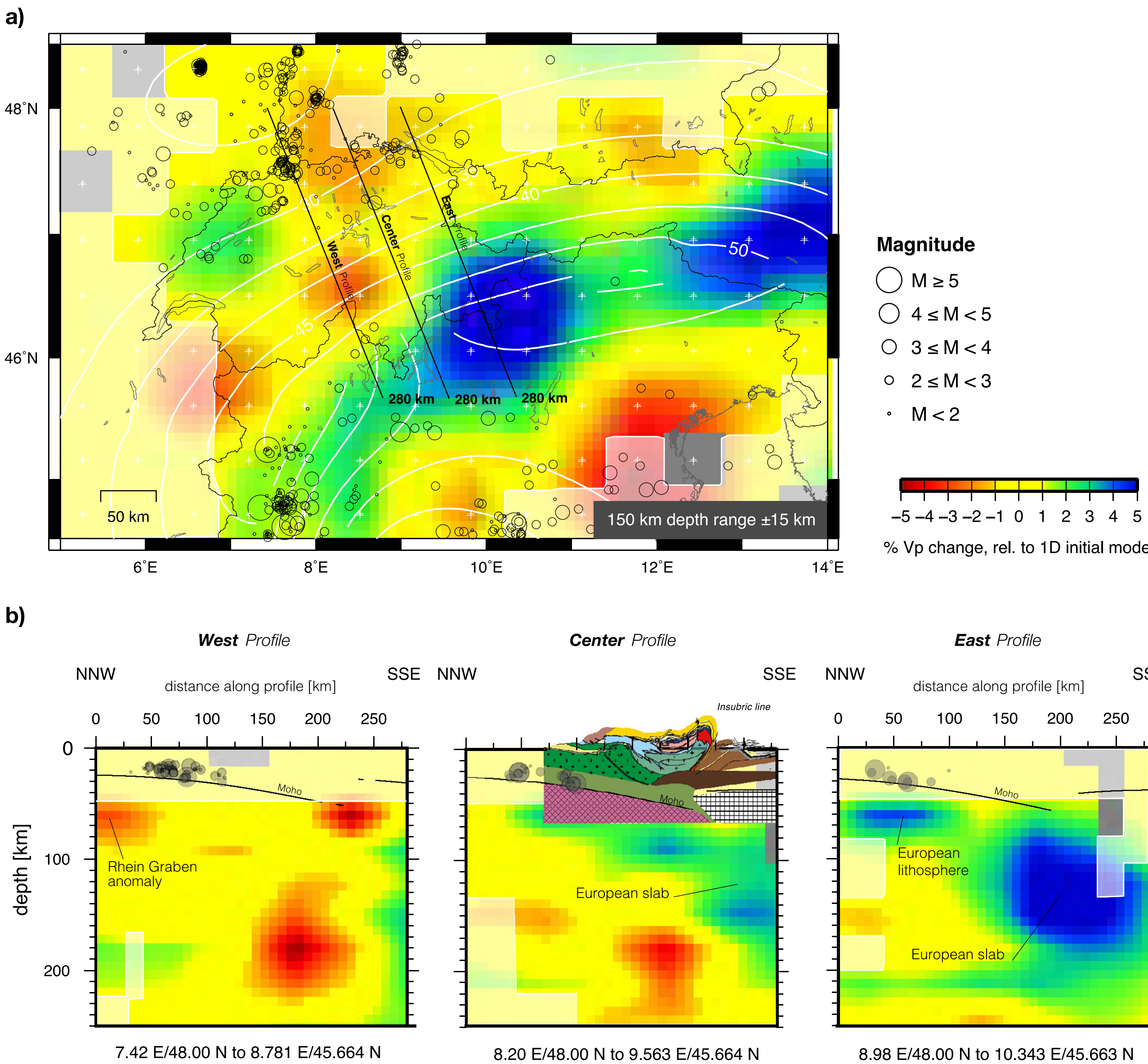

Fig. 8. Lower crustal earthquakes (black circles), Moho topography (white contour lines) and changes in P-wave velocities in the upper mantle beneath the greater Alpine region (modified from Lippitsch et al., 2003). The P-wave velocity distribution is obtained by linear interpolation between inversion cells. Velocity variations are plotted relative to a 1-D initial reference model determined from absolute travel times for this region. Areas with no ray coverage are masked with gray colors; areas with critical resolution (diagonal element of resolution matrix is smaller than 0.07) are displayed in pale colors. (a) Horizontal cross-section of teleseismic tomography between 135 km and 165 km depth. Lower crustal earthquakes within 15 km of the Moho and focal depth larger than 15 km are presented with black circles based on the EMSC earthquake catalog (January 1998–July 2011). The white contour lines represent the Moho depth (km) of the European respectively the Adriatic lithosphere (Wagner et al., 2012). White crosses indicate the grid points of the teleseismic tomography. (b) Vertical cross-sections perpendicular to strike of the Central Alps as indicated in (a). Black solid lines show the European and Adriatic Moho (Wagner et al., 2012). Lower crustal earthquakes of newly derived earthquake catalog within 30 km distance to the profile lines are presented by gray circles. Crustal structure in the Center Profile (middle) are adopted from the Bergell section in the Central Alps from (Rosenberg and Kissling, 2013).

lower continental crust (e.g. Deichmann, 1992; Maggi et al., 2000b; Jackson, 2002; Jackson et al., 2008). The assumed corset-like structure of this model is formed by thin mafic to ultramafic, sill-like intrusions and dykes with high strength surrounded by mechanically weaker, high-grade felsic rocks (Meissner and Kern, 2008). Within the strong, mafic to ultramafic network the occurrence of lower crustal earthquakes up to bulk temperatures of at least 500 °C (Weertman, 1970; Ohnaka, 1995) would be possible, if the crust was exposed to high differential stresses like those evoked by tectonic forces. Meissner and Kern (2008) assumed that the origin of this tectonic stresses is the NW–SE compression between the Adriatic and European plates. This assumption, however, disagrees with our results of a higher consistency in the orientation of the extensional T-axes than the compressional P-axes of the focal mechanisms in the northern foreland of the Central Alps (given in Kastrup et al., 2004; Deichmann, 2012; Marschall et al., 2013; Diehl et al., 2013). If the stress field of the Central Alps and its foreland were dominated by the convergence of the two plates, the orientation of the P-axes of the focal mechanism are expected to be more consistent (Fig. 7b).

The present convergence rate in the Central Alps is relatively small (1–2 mm/yr) (Calais et al., 2002; Sue et al., 2007b; D'Agostino et al., 2008) and comparable to the isostatic uplift rate (Champagnac et al., 2007; Serpelloni et al., 2013). These low convergence rates indicate a mostly locked subduction–collision zone in the Central Alps and not an ongoing dominant convergence. We correlate this post-collision tectonic state of the Central Alps and the highly consistent arc-parallel orientation of the T-axes in the

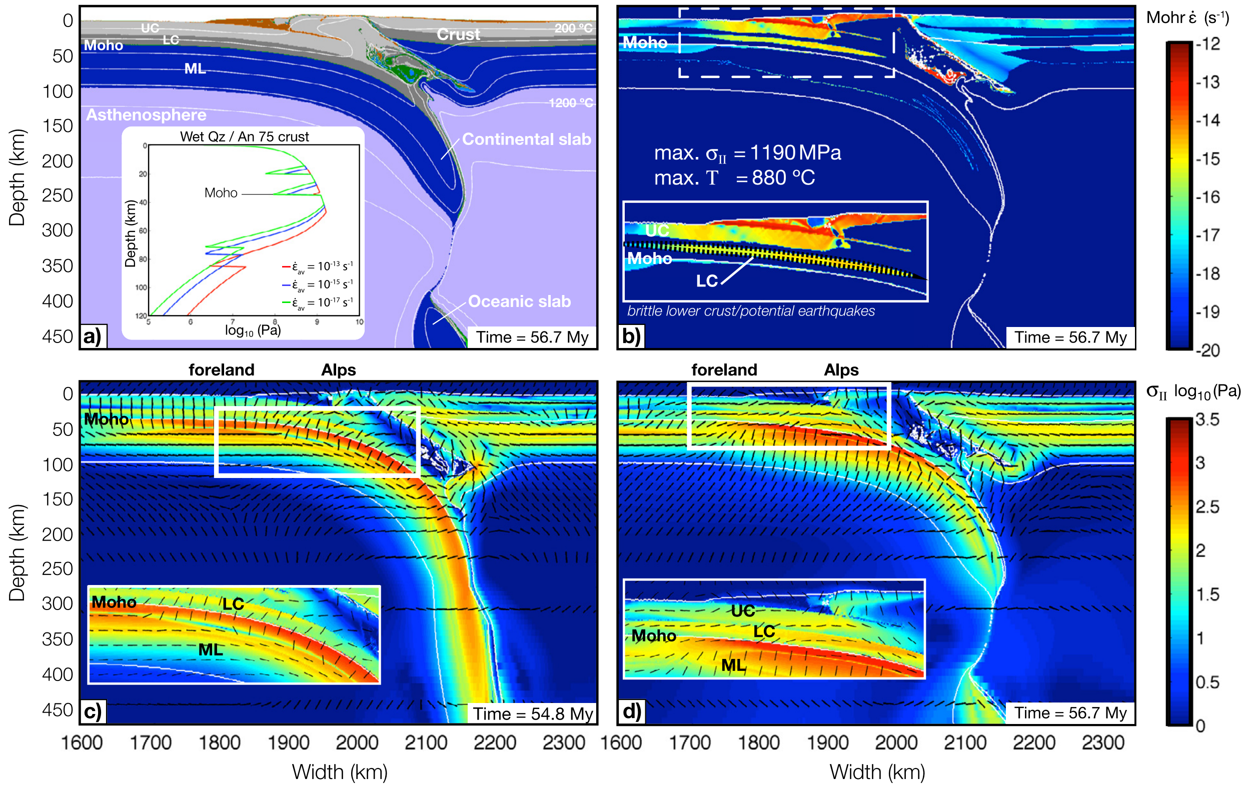

Fig. 9. 2-D thermo-mechanical model of slab detachment and rollback during continental collision using a rheologically layered crust (Duretz and Gerya, 2013). (a) Spatial distribution of lithological phases after slab detachment depicting the structure of the collision zone as well as the position of both oceanic and continental slabs. The white contours indicate isotherms (200 °C spacing), the reader is referred to Duretz and Gerya (2013) for detailed color information. UC: upper crust; LC: lower crust; ML: mantle lithosphere. (b) Location of brittle deformation (Mohr–Coulomb) after slab detachment, the colors correspond to the second strain rate invariant. The dotted line in the zoom marks the area of potential lower crustal earthquakes. Panels (c) and (d) show the time evolution of the second deviatoric stress tensor. White contours indicate lithological groups (crust, mantle lithosphere and asthenosphere) and black bars shows the orientation of the minimum principal stress (most compressive). Before detachment of the oceanic fragment, the slab is negatively buoyant and extensional stresses are thus focused within its extrados. As stresses get transmitted along the slab, the foreland is as well under an extensional state of stress (Fig. 8a). After detachment (d), the slab pull drastically diminishes whereas buoyant stresses generated by the previously subducted continental crust remains large (Duretz and Gerya, 2013). This configuration triggers concentration of compressional stresses within the lower crust in the foreland. See also movie in the online supplementary material.

European lower crust with the slab rollback model proposed by Sue et al. (1999) and Kissling (2008). In this model, the subducted European slab is pulled down by the negative buoyancy force of the mantle lithosphere, forcing the positively buoyant crust to delaminate near the Moho to form the thick crustal root (Fry et al., 2010).

The positive buoyancy force of the lower crustal root and the negative buoyancy force of the topographic load are transferred and transformed from a near vertical to a horizontal compressional stress in the foreland, orientated perpendicular to the Alpine arc (Fig. 9). The combination of the primary compressional stress axis arc-perpendicular and the secondary stress axis sub-vertical yields the arc-parallel orientation of the extensional axis. This coincides well with the observed arc-parallel orientation of the T-axes shown in Fig. 4b relating to the predominantly strike-slip faulting mechanisms. In locations where the compressional stress in the lower crust is less dominant and smaller than the vertical lithostatic stress, normal faulting is expected, but with the same arc-parallel orientation of the smallest major stress axis, the T-axis, like for the strike-slip mechanisms. Hence, the strong buoyancy forces of the crustal root and topographic load in combination with a strong dynamic coupling of the slab with its adjacent foreland as shown in Fig. 10 can explain the highly consistent orientation of the T-axes of the observed focal mechanism in combination with the occurrence of strike-slip faulting and normal faulting.

4.2. 2-D numerical models of slab rollback in a continent–continent collision

2-D thermo-mechanical modeling of a continent–continent collision (Fig. 9) including specific rheologies for the major layers of the continental lithosphere (Duretz and Gerya, 2013) suggests enhanced tectonic stresses in the subducting plate transferred from the subduction zone to the foreland. In these numerical models, where continental lithosphere is subducted beneath another continental lithosphere in a continent–continent collision, dynamics are driven only by internal body forces without additional compressional forces after the collision started (Duretz and Gerya, 2013). This allows modeling more realistic dynamics and corresponding tectonic stresses of subduction slab rollback and slab break-off mechanisms. Originally, the predominant forces are slab pull of the subducting oceanic lithosphere. When the continental lithosphere (like the European lithosphere) enters the subduction zone, the system changes to a continent–continent collision and the subduction becomes almost stagnant with the oceanic lithosphere slab strongly pulling at the continental lithosphere and forcing the subducted continental crust to delaminate from the mantle lithosphere.

Prior to the detachment of the subducted oceanic mantle slab from the continental slab, the entire slab dips nearly vertically into the asthenosphere (Fig. 9c). High stresses are focused in the mantle lithosphere of the subduction zone. Beneath the foreland both crustal layers are influenced by the slab and show elevated

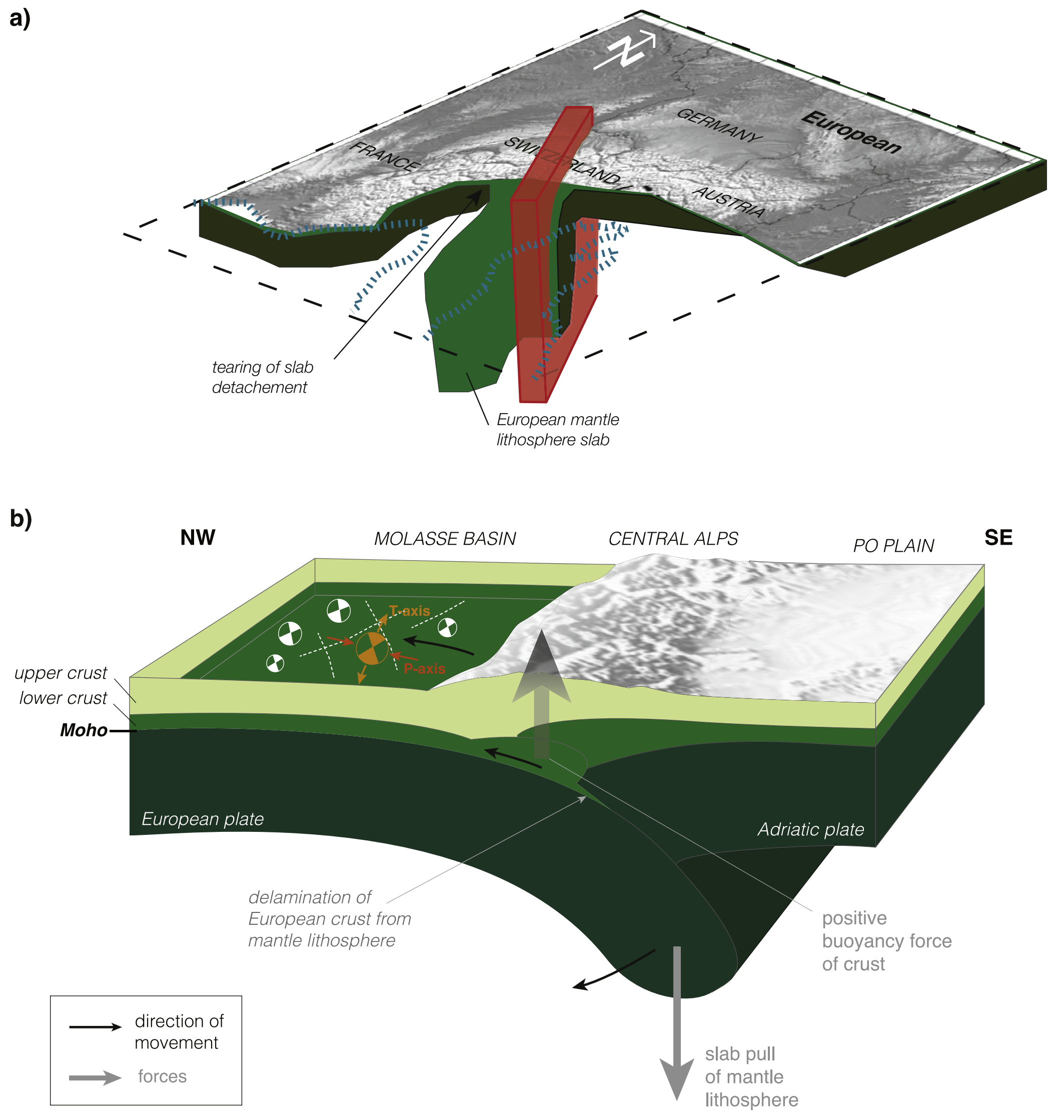

Fig. 10. Conceptual models of large-scale structures and their dynamics in the Alpine arc and in particular in the Central Alps. (a) 3-D model of European lithosphere structure in the Alpine arc based on mantle tomography (Lippitsch et al., 2003), the Adriatic plate in the South is not shown. The European lithosphere is presented by the dark green plate. The dashed blue line indicates the coastline of the Mediterranean Sea and the red box the cross-section of the model in (b). (b) Sketch of rollback of the European slab beneath Central Europe, the corresponding tectonic forces (gray arrows) and stresses (black arrows). White dashed lines indicate potential fracture patterns and white 'beach balls' show potential focal mechanisms in top view. The colored 'beach ball' demonstrates the associated orientation of the T-/P-axes for the predominant strike-slip mechanisms.

stresses, however they are significantly lower than for the strong underlying mantle lithosphere. Such a geometry of a nearly vertical 170 km long slab is expected at 10°E beneath the eastern end of the Central Alps (Fig. 8a and Lippitsch et al., 2003). In the northern foreland of this region (in South Germany) lower crustal earthquakes occur based on the EMSC catalog (Figs. 1 and 8a), but less regularly compared to the Swiss foreland further east.

Eventually, the oceanic part of the slab detaches and thus the slab pull is significantly reduced. This almost immediately causes a major change in the stress regime in the continental (European) plate reaching well into the foreland (see movie in the online supplementary material). After the detachment of the oceanic slab from the continental mantle slab at around 300 km depth, the stresses in the crust and mantle lithosphere are higher and the lithospheric slab dips less steep into the asthenosphere (Figs. 9a, 9b and 9d). In this stage of the continent subduction with slab rollback, the yield strength of the Mohr–Coulomb plasticity in parts of the lower and upper crust is exceeded as shown in Fig. 9b. This coincides with the peculiar occurrence of lower crustal earthquakes within 100 km of the northern front of the Central Alps shown by the EMSC locations in Fig. 8 and the high-precision relocations in Fig. 4a.

In Figs. 9b and 9d the numerical models show a strong, dynamic coupling of the subducted lithospheric with the adjacent foreland for stresses and strain rates which confirms the proposed stress transfer from the orogenic root towards the foreland (Fig. 10). The dynamic coupling is more pronounced for the gently to steeply and shorter slab, and agrees with the variable intensity of the lower crustal seismicity represented in the EMSC catalog in the northern foreland of the Central Alps and the Central to Eastern Alps. Moreover, for the nearly vertically long dipping slab the compressional stress axes in the foreland are neither horizontal nor arc-perpendicular like shown by the focal mechanisms (Fig. 4b), instead the foreland and the bending slab show a consistent extensional stress pattern (Fig. 9c) like observed in the shallow Benioff–Wadati of a typically oceanic lithosphere subduction beneath southern Alaska (Kissling and Lahr, 1991). After the detachment of the oceanic fragment and the initiation of the slab rollback, the slab pull drastically diminishes whereas buoyant stresses generated by the previously subducted continental crust remains large (Duretz and Gerya, 2013) and transmitted as compressional stress to the foreland (horizontal alignment of major compressional stress axis in Fig. 9b, see also movie in the online supplementary material). This coincides well with the orientation of the P-/T-axes of the observed focal mechanisms and emphasize the importance and influence of the slab rollback mechanism on the regional stress field in the foreland.

The lithospheric rheology of the 2-D numerical models is strongly simplified and does not reflect the proposed complex, high-strength network of the European lower crust composed of a mafic to ultramafic material (Holliger and Levander, 1994; Meissner and Kern, 2008). In the numerical models, the upper crust is composed of quartzite with an underlying lower crust of plagioclase (An75) and a peridotitic mantle (Fig. 9a) (Duretz and Gerya, 2013). The brittle yield-strength according to the Mohr–Coulomb criteria (Fig. 9b) in the upper mantle lithosphere of the 2-D models, however, is not reached and no mantle earthquakes are expected, which agrees well with our high-precision hypocenter locations. In the mantle lithosphere the resulting strain rate ($\sim$10–20 s^{-1}) is five orders of magnitude lower than in the lower crust ($\sim$10–15 s^{-1}) despite the stress being one magnitude larger. For the peridotitic mantle the brittle yield strength is significantly higher. Moreover, the transition to a ductile behavior of the lower crust in the subduction zone at around 35 km depth (Fig. 9b) agrees well with the observed shutdown of lower crustal seismicity beneath the Alpine front as shown by our relocations in Fig. 4b.

Although the numerical models are limited to two-dimensions, the assessment of comprehensive stresses and strain rates within the subducted lithosphere and the adjacent lithosphere in the foreland of the Central Alps caused by the slab rollback are representative. The gently to steeply dipping European slab beneath the Central Alps represents a large-scale regional structure as shown in Fig. 8a, with a width of around 100 km in the complex 3-D lithospheric geometry of the Alpine arc.

In comparison to the imaged geometry and size of the European slab beneath the Central Alps (Lippitsch et al., 2003), the length of the continental slab after the detachment of the oceanic part (Figs. 9a, b and d) is around 100 km longer. Nevertheless, the additional weight of the slab in the 2-D models can be assigned to the respective weight of the attached part of European slab in the West. This part of the European slab is already detached from the upper lithospheric structures of the Western Alps (Fig. 8a) and is only connected to the slab in the Central Alps (Lippitsch et al., 2003). Besides this spatial representativeness of the numerical models, the duration of the oceanic subduction, lasting for 40 Ma and the following onset of the continent–continent collision in general agrees with the approximate evolution of the Alpine collision (Schmid and Kissling, 2000).

The geographical distribution of earthquakes in the lower crust of the northern Alpine foreland and the absence of seismicity in the underlying mantle lithosphere corresponds well with the model of stress transfer from a slab rollback of the European slab in the Central Alpine subduction zone into the northern foreland (Fig. 8). The relative moderate bending of the European lithosphere under significant load and a strong opposing buoyant stress implies a significantly high elastic strength of the mantle lithosphere and a strong mechanical coupling of the lower crust to the mantle lithosphere.

4.3. *Focal depth distribution related to lower crustal characteristics*

Besides the confirmation of an aseismic European mantle, the systematic high-precision relocation reveals a rather homogeneous depth distribution of lower crustal earthquakes beneath the northern foreland of the Central Alps with a possible exception of clustering at the transition zone between upper and lower crust. The observed clustering of the 104 precisely relocated earthquakes at the Conrad discontinuity, if taken as representative for all 471 lower crustal earthquakes in this region, might indicate the less strong mechanical coupling of the two crustal layers. In addition, an enhancement of metamorphic processes related to α–β quartz transition in metapelites (Zappone and Benson, 2013) at this depth might be possible and promote brittle failure respective the occurrence of earthquakes. Our relocations further confirm individual earthquake clusters with similar fault planes in the lower crust (Figs. 4 and 7) suggesting a possible interrelation among those earthquakes. Another reason for the clustering could be the presence of high-pressure fluids in the lower European crust. Additional evidence for high-pressure fluids are relatively low P-wave velocities of 6.2–6.4 km/s in the lower crust (Holliger and Kissling, 1992; Ye et al., 1995; Diehl et al., 2009a). Based on petrophysical laboratory experiments the relatively low P-wave velocities could be assigned to the presence of fluids from dehydration reaction of metapelites (Zappone et al., 2006). The high strength of the mafic to ultramafic network in the lower European crust proposed by Meissner and Kern (2008) is compatible with high-pressure fluids, which might enhance plastic instabilities between the highly heterogeneous layers of the network and the relatively weak surrounding lower crust. Due to the multiple and irregularly aligned layers of sill-like intrusions (Meissner and Kern, 2008), the locations of earthquakes are expected to occur at variable depths throughout the lower crust. Nevertheless, the occurrence of small local earthquake clusters is likely. At the Rhine Graben around Basel with its inherited, pre-existing deep crustal faults an interaction of these graben structures with the transferred tectonic stresses from the subducted European slab might lead to the enhanced lower crustal seismicity in this region.

5. Conclusions

High-precision hypocenter locations of lower crustal earthquakes and focal mechanism characteristics beneath the northern Alpine foreland of the Central Alps in combination with numerical models of continent–continent subduction show a strong correlation of the occurrence of these earthquakes with large-scale geodynamic processes. Deep earthquakes beneath the northern Alpine foreland of the Central Alps are confined to the lower crust and their geographical distribution correlates well with the lateral extension of the gently to steeply dipping European slab beneath the Central Alps. The subducted European slab beneath the Central Alps has a length of about 120 km (Lippitsch et al., 2003) that controls the post-collisional large-scale lithospheric dynamics of the Alps by slab rollback. Based on 2-D numerical modeling, we propose a dynamic coupling and stress transfer in the lithosphere from the slab, crustal root and topographic load beneath the Alps to the northern foreland. Such a tectonic stress transfer leads to a locally enhanced regional stress field in the lower and upper crust beneath the foreland with a compressional component perpendicular and an extensional component parallel to the strike of the Central Alps. This agrees well with the consistent T- and P-axes patterns in the foreland of the Central Alps and with the proposed mafic to ultramafic 'corset' model for the lower European crust by Holliger and Levander (1994) and Meissner and Kern (2008). The presence of high-pressure fluids in the lower crust seems likely and in combination with the high strength network it would explain the peculiar rheological characteristics of the lower European crust. The key role in the occurrence of lower crustal seismicity in the northern foreland of the Alpine arc, however, seems to be the stress transfer from the European slab into the foreland.

Acknowledgements

We thank N. Deichmann for providing his focal mechanism catalog and helpful background information. For constructive comments and discussions we thank S. Schmid, N. Deichmann, T. Gerya and A. Zappone. Comments by two anonymous reviewers significantly improved the manuscript. We thankfully acknowledge continuous support of the Swiss Seismological Service.

Appendix A. Supplementary material

Supplementary material related to this article can be found online at http://dx.doi.org/10.1016/j.epsl.2014.04.002.

References

Calais, E., Nocquet, J.-M., Jouanne, F., Tardy, M., 2002. Current strain regime in the Western Alps from continuous Global Positioning System measurements, 1996–2001. Geology 30, 651–654. http://dx.doi.org/10.1130/0091-7613(2002)030<0651:CSRITW>2.0.CO;2. http://geology.gsapubs.org/content/30/7/651.abstract. arXiv:http://geology.gsapubs.org/content/30/7/651.full.pdf+html.

Champagnac, J., Molnar, P., Anderson, R., Sue, C., Delacou, B., 2007. Quaternary erosion-induced isostatic rebound in the western Alps. Geology 35, 195–198. http://dx.doi.org/10.1130/G23053A.1. http://geology.gsapubs.org/content/35/3/195.abstract. arXiv:http://geology.gsapubs.org/content/35/3/195.full.pdf+html.

Chen, W.-P., 1988. A brief update on the focal depths of intracontinental earthquakes and their correlations with heat flow and tectonic age. Seismol. Res. Lett. 59, 263–272.

Chen, W.-P., Molnar, P., 1983. Focal depths of intracontinental and intraplate earthquakes and their implications for the thermal and mechanical properties of the lithosphere. J. Geophys. Res., Solid Earth 88, 4183–4214. http://dx.doi.org/10.1029/JB088iB05p04183.

Chen, W.-P., Hung, S.-H., Tseng, T.-L., Brudzinski, M., Yang, Z., Nowack, R.L., 2012. Rheology of the continental lithosphere: progress and new perspectives. Gondwana Res. 21, 4–18. http://www.sciencedirect.com/science/article/pii/S1342937X1100205X.

D'Agostino, N., Avallone, A., Cheloni, D., D'Anastasio, E., Mantenuto, S., Selvaggi, G., 2008. Active tectonics of the Adriatic region from GPS and earthquake slip vectors. J. Geophys. Res., Solid Earth 113. http://dx.doi.org/10.1029/2008JB005860.

Deichmann, N., 1987. Focal depths of earthquakes in northern Switzerland. Ann. Geophys., Ser. B, Terr. Planet. Phys. 5B, 395–402.

Deichmann, N., 1992. Structural and rheological implications of lower-crustal earthquakes below northern Switzerland. Phys. Earth Planet. Inter. 69, 270–280. http://www.sciencedirect.com/science/article/pii/003192019290146M.

Deichmann, N., 2012. Earthquakes in Switzerland and surrounding regions. Annual Reports 1996–2011, http://www.seismo.ethz.ch/prod/j_reports/index.

Deichmann, N., Rybach, L., 1989. Earthquakes and temperatures in the lower crust below the northern alpine foreland of Switzerland. In: Properties and Processes of Earth's Lower Crust, vol. 51. AGU, Washington, DC, pp. 197–213. http://dx.doi.org/10.1029/GM051p0197.

Deichmann, N., Baer, M., Braunmiller, J., Ballarin Dolfin, D., Bay, F., Delouis, B., Fäh, D., Giardini, D., Kastrup, U., Kind, F., Kradolfer, U., Künzle, W., Röthlisberger, S., Schler, T., Salichon, J., Sellami, S., Spühler, E., Wiemer, S., 1999. Earthquakes in Switzerland and surrounding regions during 1999. Eclogae Geol. Helv. 93, 395–406.

Delacou, B., Sue, C., Champagnac, J.-D., Burkhard, M., 2004. Present-day geodynamics in the bend of the western and central Alps as constrained by earthquake analysis. Geophys. J. Int. 158, 753–774. http://dx.doi.org/10.1111/j.1365-246X.2004.02320.x.

Dèzes, P., Schmid, S.M., Ziegler, P.A., 2004. Evolution of the European Cenozoic Rift System: interaction of the Alpine and Pyrenean orogens with their foreland lithosphere. Tectonophysics 389, 1–33. http://dx.doi.org/10.1016/j.tecto.2004.06.011. http://www.sciencedirect.com/science/article/pii/S0040195104001957.

Diehl, T., Husen, S., Kissling, E., Deichmann, N., 2009a. High-resolution 3-D P-wave model of the Alpine crust. Geophys. J. Int. 179, 1133–1147. http://dx.doi.org/10.1111/j.1365-246X.2009.04331.x.

Diehl, T., Kissling, E., Husen, S., Aldersons, F., 2009b. Consistent phase picking for regional tomography models: application to the greater Alpine region. Geophys. J. Int. 176, 542–554. http://dx.doi.org/10.1111/j.1365-246X.2008.03985.x.

Diehl, T., Deichmann, N., Clinton, J., Husen, S., Kraft, T., Plenkers, K., Edwards, B., Cauzzi, C., Michel, C., Kästli, P., Wiemer, S., Haslinger, F., Fäh, D., Kradolfer, U., Woessner, J., 2013. Earthquakes in Switzerland and surrounding regions during 2012. Swiss J. Geosci. 106, 543–558. http://dx.doi.org/10.1007/s00015-013-0154-4.

Duretz, T., Gerya, T., 2013. Slab detachment during continental collision: influence of crustal rheology and interaction with lithospheric delamination. Tectonophysics 602, 124–140. http://dx.doi.org/10.1016/j.tecto.2012.12.024. http://www.sciencedirect.com/science/article/pii/S0040195113000061.

Engdahl, E.R., van der Hilst, R., Buland, R., 1998. Global teleseismic earthquake relocation with improved travel times and procedures for depth determination. Bull. Seismol. Soc. Am. 88, 722–743. http://www.bssaonline.org/content/88/3/722.abstract. arXiv:http://www.bssaonline.org/content/88/3/722.full.pdf+html.

Fäh, D., Giardini, D., Kästli, P., Deichmann, N., Gisler, M., Schwarz-Zanetti, G., Alvarez-Rubio, S., Sellami, S., Edwards, B., Allmann, B., Bethmann, F., Wössner, J., Gassner-Stamm, G., Fritsche, S., Eberhard, D., 2011. ECOS-09 Earthquake catalogue of Switzerland. Release 2011 Report and Database. Public catalogue, 17.4.2011. Swiss Seismological Service, ETH Zurich.

Fry, B., Deschamps, F., Kissling, E., Stehly, L., Giardini, D., 2010. Layered azimuthal anisotropy of Rayleigh wave phase velocities in the European Alpine lithosphere inferred from ambient noise. Earth Planet. Sci. Lett. 297, 95–102. http://www.sciencedirect.com/science/article/pii/S0012821X10003821.

Garcia Fernandez, M., Mayer-Rosa, D., 1986. Improved hypocentral parameter determination using secondary regional phases. Rev. Geophys. 42, 175–184.

Godey, S., Bossu, R., Guilbert, J., Mazet-Roux, G., 2006. The Euro-Mediterranean bulletin: a comprehensive seismological bulletin at regional scale. Seismol. Res. Lett. 77, 460–474. http://srl.geoscienceworld.org/content/77/4/460.short.

Holliger, K., Kissling, E., 1992. Gravity interpretation of a unified 2-D acoustic image of the central Alpine collision zone. Geophys. J. Int. 111, 213–225. http://dx.doi.org/10.1111/j.1365-246X.1992.tb00571.x.

Holliger, K., Levander, A., 1994. Lower crustal reflectivity modeled by rheological controls on mafic intrusions. Geology 22, 367–370. http://dx.doi.org/10.1130/0091-7613(1994)022<0367:LCRMBR>2.3.CO;2. http://geology.gsapubs.org/content/22/4/367.abstract. arXiv:http://geology.gsapubs.org/content/22/4/367.full.pdf+html.

Husen, S., Kissling, E., Deichmann, N., Wiemer, S., Giardini, D., Baer, M., 2003. Probabilistic earthquake location in complex three-dimensional velocity models: application to Switzerland. J. Geophys. Res., Solid Earth 108, 2077. http://dx.doi.org/10.1029/2002JB001778.

Jackson, J., 2002. Strength of the continental lithosphere: time to abandon the jelly sandwich? GSA Today 12, 4. http://dx.doi.org/10.1130/1052-5173(2002)012<0004:SOTCLT>2.0.CO;2.

Jackson, J., McKenzie, D., Priestley, K., Emmerson, B., 2008. New views on the structure and rheology of the lithosphere. J. Geol. Soc. 165, 453–465. http://dx.doi.org/10.1144/0016-76492007-109. http://jgs.lyellcollection.org/content/165/2/453.abstract. arXiv:http://jgs.lyellcollection.org/content/165/2/453.full.pdf+html.

Kastrup, U., Deichmann, N., Fröhlich, A., Giardini, D., 2007. Evidence for an active fault below the northwestern Alpine foreland of Switzerland. Geophys. J. Int. 169, 1273–1288. http://dx.doi.org/10.1111/j.1365-246X.2007.03413.x.

Kastrup, U., Zoback, M.L., Deichmann, N., Evans, K.F., Giardini, D., Michael, A.J., 2004. Stress field variations in the Swiss Alps and the northern Alpine foreland derived from inversion of fault plane solutions. J. Geophys. Res., Solid Earth 109, B01402. http://dx.doi.org/10.1029/2003JB002550.

Kissling, E., 2008. Deep structure and tectonics of the Valais – and the rest of the Alps. Bull. Angew. Geol. 13, 3–10. http://www.scopus.com/inward/record.url?eid=2-s2.0-69549118960&partnerID=40&md5=3fd955aaaa4c8560d952e351fc89d0fc.

Kissling, E., Husen, S., Haslinger, F., 2001. Model parametrization in seismic tomography: a choice of consequence for the solution quality. Phys. Earth Planet. Inter. 123, 89–101. http://dx.doi.org/10.1016/S0031-9201(00)00203-X. http://www.sciencedirect.com/science/article/pii/S003192010000203X.

Kissling, E., Lahr, J.C., 1991. Tomographic image of the Pacific Slab under southern Alaska. Eclogae Geol. Helv. 84, 297–316.

Kissling, E., Deichmann, N., Husen, S., Zappone, A., 2006a. Lower crustal seismic velocities and seismicity in the northern Alpine foreland: II. Geodynamical interpretation. In: Geophys. Res. Abstr., vol. 8. 04444, European Geosciences Union.

Kissling, E., Schmid, S.M., Lippitsch, R., Ansorge, J., Fügenschuh, B., 2006b. Lithosphere structure and tectonic evolution of the Alpine arc: new evidence from high-resolution teleseismic tomography. Mem. Geol. Soc. Lond. 32, 129–145. http://dx.doi.org/10.1144/GSL.MEM.2006.032.01.08. http://mem.lyellcollection.org/content/32/1/129.abstract. arXiv:http://mem.lyellcollection.org/content/32/1/129.full.pdf+html.

Leclère, H., Daniel, G., Fabbri, O., Cappa, F., Thouvenot, F., 2013. Tracking fluid pressure buildup from focal mechanisms during the 2003–2004 Ubaye seismic swarm, France. J. Geophys. Res. Solid Earth 118, 4461–4476. http://dx.doi.org/10.1002/jgrb.50297.

Lippitsch, R., Kissling, E., Ansorge, J., 2003. Upper mantle structure beneath the Alpine orogen from high-resolution teleseismic tomography. J. Geophys. Res., Solid Earth 108, 2376. http://dx.doi.org/10.1029/2002JB002016.

Lomax, A., 2005. A reanalysis of the hypocentral location and related observations for the great 1906 California earthquake. Bull. Seismol. Soc. Am. 95, 861–877. http://dx.doi.org/10.1785/0120040141. http://www.bssaonline.org/content/95/3/861.abstract. arXiv:http://www.bssaonline.org/content/95/3/861.full.pdf+html.

Lomax, A., Virieux, J., Volant, P., Thierry-Berge, C., 2000. Probabilistic earthquake location in 3D and layered models. In: Advances in Seismic Event Location, pp. 101–134. http://books.google.ch/books?id=wIBMjf_fWTIC.

Lombardi, D., Braunmiller, J., Kissling, E., Giardini, D., 2008. Moho depth and Poisson's ratio in the Western–Central Alps from receiver functions. Geophys. J. Int. 173, 249–264. http://dx.doi.org/10.1111/j.1365-246X.2007.03706.x.

Maggi, A., Jackson, J.A., McKenzie, D., Priestley, K., 2000a. Earthquake focal depths, effective elastic thickness, and the strength of the continental lithosphere. Geology 28, 495–498. http://geology.gsapubs.org/content/28/6/495.abstract.

Maggi, A., Jackson, J.A., Priestley, K., Baker, C., 2000b. A re-assessment of focal depth distributions in southern Iran, the Tien Shan and northern India: do earthquakes really occur in the continental mantle? Geophys. J. Int. 143, 629–661. http://dx.doi.org/10.1046/j.1365-246X.2000.00254.x.

Marschall, I., Deichmann, N., Marone, F., 2013. Earthquake focal mechanisms and stress orientations in the eastern Swiss Alps. Swiss J. Geosci. 106, 1–12. http://dx.doi.org/10.1007/s00015-013-0129-5.

Meissner, R., Kern, H., 2008. Earthquakes and strength in the laminated lower crust – can they be explained by the "corset model"? Tectonophysics 448, 49–59. http://dx.doi.org/10.1016/j.tecto.2007.11.034. http://www.sciencedirect.com/science/article/pii/S0040195107003873.

Ohnaka, M., 1995. A shear failure strength law of rock in the brittle-plastic transition regime. Geophys. Res. Lett. 22, 25–28. http://dx.doi.org/10.1029/94GL02791.

Okaya, N., Freeman, R., Kissling, E., Mueller, S., 1996. A lithospheric cross-section through the Swiss Alps—I. Thermokinematic modelling of the Neoalpine orogeny. Geophys. J. Int. 125, 504–518. http://dx.doi.org/10.1111/j.1365-246X.1996.tb00014.x.

Quin, H.R., Thurber, C.H., 1992. Seismic velocity structure and event relocation in Kazakhstan from secondary P phases. Bull. Seismol. Soc. Am. 82, 2494–2510. http://www.bssaonline.org/content/82/6/2494.abstract. arXiv:http://www.bssaonline.org/content/82/6/2494.full.pdf+html.

Rawlinson, N., Sambridge, M., 2004. Wave front evolution in strongly heterogeneous layered media using the fast marching method. Geophys. J. Int. 156, 631–647. http://dx.doi.org/10.1111/j.1365-246X.2004.02153.x.

Rosenberg, C.L., Kissling, E., 2013. Three-dimensional insight into Central-Alpine collision: lower-plate or upper-plate indentation?. Geology 41, 1219–1222. http://dx.doi.org/10.1130/G34584.1. http://geology.gsapubs.org/content/41/12/1219.abstract. arXiv:http://geology.gsapubs.org/content/41/12/1219.full.pdf+html.

Schmid, S.M., Kissling, E., 2000. The arc of the western Alps in the light of geophysical data on deep crustal structure. Tectonics 19, 62–85. http://dx.doi.org/10.1029/1999TC900057.

Scholz, C., 2002. The Mechanics of Earthquakes and Faulting. Cambridge University Press. http://books.google.ch/books?id=JL1VM5wMbrQC.

Serpelloni, E., Faccenna, C., Spada, G., Dong, D., Williams, S.D.P., 2013. Vertical GPS ground motion rates in the Euro–Mediterranean region: new evidence of velocity gradients at different spatial scales along the Nubia-Eurasia plate boundary. J. Geophys. Res., Solid Earth 118, 6003–6024. http://dx.doi.org/10.1002/2013JB010102.

Sue, C., Thouvenot, F., Fréchet, J., Tricart, P., 1999. Widespread extension in the core of the western Alps revealed by earthquake analysis. J. Geophys. Res. 104, 25611–25622. http://dx.doi.org/10.1029/1999JB900249.

Sue, C., Delacou, B., Champagnac, J.-D., Allanic, C., Burkhard, M., 2007a. Aseismic deformation in the Alps: GPS vs. seismic strain quantification. Terra Nova 19, 182–188. http://dx.doi.org/10.1111/j.1365-3121.2007.00732.x.

Sue, C., Delacou, B., Champagnac, J.-D., Allanic, C., Tricart, P., Burkhard, M., 2007b. Extensional neotectonics around the bend of the Western/Central Alps: an overview. Int. J. Earth Sci. 96, 1101–1129. http://dx.doi.org/10.1007/s00531-007-0181-3.

Wagner, M., Kissling, E., Husen, S., 2012. Combining controlled-source seismology and local earthquake tomography to derive a 3-D crustal model of the western Alpine region. Geophys. J. Int. 191, 789–802. http://dx.doi.org/10.1111/j.1365-246X.2012.05655.x.

Wagner, M., Husen, S., Lomax, A., Kissling, E., Giardini, D., 2013. High-precision earthquake locations in Switzerland using regional secondary arrivals in a 3-D velocity model. Geophys. J. Int. 193, 1589–1607. http://dx.doi.org/10.1093/gji/ggt052. http://gji.oxfordjournals.org/content/193/3/1589.abstract. arXiv:http://gji.oxfordjournals.org/content/193/3/1589.full.pdf+html.

Waldhauser, F., Kissling, E., Ansorge, J., Mueller, S., 1998. Three-dimensional interface modelling with two-dimensional seismic data: the Alpine crust–mantle boundary. Geophys. J. Int. 135, 264–278. http://dx.doi.org/10.1046/j.1365-246X.1998.00647.x.

Waldhauser, F., Lippitsch, R., Kissling, E., Ansorge, J., 2002. High-resolution teleseismic tomography of upper-mantle structure using an a priori three-dimensional crustal model. Geophys. J. Int. 150, 403–414. http://dx.doi.org/10.1046/j.1365-246X.2002.01690.x.

Weertman, J., 1970. The creep strength of the earth's mantle. Rev. Geophys. 8, 145–168. http://dx.doi.org/10.1029/RG008i001p00145.

Wilson, M., Downes, H., 2006. Tertiary–Quaternary intra-plate magmatism in Europe and its relationship to mantle dynamics. Mem. Geol. Soc. Lond. 32, 147–166. http://mem.lyellcollection.org/content/32/1/147.abstract.

Ye, S., Ansorge, J., Kissling, E., Mueller, S., 1995. Crustal structure beneath the eastern Swiss Alps derived from seismic refraction data. Tectonophysics 242, 199–221. http://dx.doi.org/10.1016/0040-1951(94)00209-R. http://www.sciencedirect.com/science/article/pii/004019519400209R.

Zappone, A.S., Benson, P.M., 2013. Effect of phase transitions on seismic properties of metapelites: a new high-temperature laboratory calibration. Geology 41, 463–466. http://dx.doi.org/10.1130/G33713.1. http://geology.gsapubs.org/content/41/4/463.abstract.

Zappone, A., Burlini, L., Connolly, J., Husen, S., Kissling, E., 2006. Lower crustal seismic velocities and seismicity in the northern Alpine foreland: I. Observations and petrophysical experiments. In: Geophys. Res. Abstr., vol. 8. 04381, European Geosciences Union.